

Numerical Modeling of Spatial Permafrost Dynamics in Alaska

Sergei Marchenko

Geophysical Institute, University of Alaska Fairbanks, USA

Vladimir Romanovsky

Geophysical Institute, University of Alaska Fairbanks, USA

Gennady Tipenko

Institute of Geoecology, Russian Academy of Science, Russia

Abstract

The Geophysical Institute Permafrost Laboratory model (GIPL) simulates soil temperature dynamics and the depth of seasonal freezing and thawing by solving 1D non-linear heat equation with phase change numerically. In this model the process of soil freezing/thawing is occurring in accordance with the unfrozen water content curve and soil thermal properties, which are specific for each soil layer and for each geographical location. At the present stage of development, the GIPL 2.0 model is combined with ArcGIS to facilitate preparation of input parameters and visualization of simulated results in a form of digital maps. The future climate scenario was derived from the Massachusetts Institute of Technology MIT-2D climate model output for the 21st century. This climate scenario was used as a driving force in GIPL model. Initial results of calculations show that by the end of the current century the widespread permafrost degradation could begin everywhere in Alaska southward from the Brooks Range.

Keywords: Active Layer Thickness; Ground Temperature; Numerical Modeling; Thawing Permafrost;

Introduction

Many components of the Cryosphere, particularly sea ice, glaciers and permafrost, react sensitively to climate change. Climatic changes and changes in permafrost were reported recently from many regions of the Northern Hemisphere (Jin et al 2000, Oberman & Mazhitova 2001, Harris & Haerberli 2003, Sharkhuu 2003, Romanovsky et al. 2002, Marchenko et al. 2007). Significant changes in permafrost temperatures were observed in Alaska. Ground temperature data from Alaska available for the last 30 years demonstrate an increase in permafrost temperatures by 0.5-3°C (Osterkamp & Romanovsky 1999, Osterkamp 2005). Recent observations show that the warming of permafrost has continued into the 21st century in Alaska (Clow & Urban 2002, Romanovsky et al. 2002, Romanovsky et al. 2003). While the increase in permafrost temperature may change many of its physical properties, the major threshold occurs when permafrost starts to thaw from its top down. The thawing and freezing of soils in Arctic and sub-Arctic regions is affected by many factors, with air temperature, vegetation, snow accumulation, and soil moisture among the most significant. To investigate how observed and projected changes in these factors influence permafrost dynamics in Alaska, we developed a numerical Geophysical Institute Permafrost Laboratory (GIPL) model. In this paper we will first describe this model. Then we will show how this model should be calibrated and validated before it could be used for projections of future changes in permafrost as a result of changes in climatic and other environmental conditions. After validation, the model was used to develop one possible scenario of the permafrost dynamics in Alaska during the current century.

Previous spatial modeling of permafrost

Recently, there have been a number of experiments to simulate soil temperature and permafrost dynamics on regional and global scales (Anisimov & Nelson 1997, Stendel & Christensen 2002, Sazonova & Romanovsky 2003, Oelke & Zhang 2004, Lawrence & Slater 2005, Zhang et al. 2006, Saito et al. 2007). There are two major approaches to spatial modeling of permafrost. One of them is to include a permafrost module directly into GCM. The second one employs the use of stand-alone equilibrium or transient permafrost models. These models are forced by the climatic outputs produced by GCMs. There were a few examples of simulations and forecasts of permafrost dynamics using coupled global climate models (Stendel & Christensen 2002, Lawrence & Slater 2005, Nicolsky et al. 2007, Saito et al. 2007), but some of the modeled results generated a significant controversy (Burn & Nelson 2006, Delisle 2007). The simplified treatment of subsurface thermal processes and problematic settings of the soil properties and lower boundary conditions precluded proper representation of the future permafrost dynamics in these GCMs (Burn & Nelson 2006).

In this research we used the GIPL-2.0 model, which is a numerical simulator of the temporal and spatial transient response of permafrost to projected changes in climate.

Methods

GIPL-2.0 Model

Previous version of this model (GIPL-1.0) is equilibrium, spatially distributed, analytical model for computation of the active layer thickness and mean annual ground temperatures (Sazonova & Romanovsky 2003). The GIPL-2.0 model simulates soil temperature dynamics and the depth of seasonal freezing and thawing by solving 1D non-

linear heat equation with phase change numerically. In this model the process of soil freezing/thawing is occurring in accordance with the unfrozen water content curve and soil thermal properties, which are specific for each soil layer and for each geographical location. Special Enthalpy formulation of the energy conservation law makes it possible to use a coarse vertical resolution without loss of latent heat effects in phase transition zone even in case of fast temporally and spatially varying temperature fields. At the present stage of development, the GIPL model is combined with ArcGIS to facilitate preparation of input parameters (climate forcing from observations or from Global or Regional Climate Models) and visualization of simulated results in a form of digital maps. The input data are incorporated into GIS and contains the information on geology, soils properties, vegetation, air temperature, and snow distribution (Figure 1).

The soil characterization used in the GIPL-2.0 model is based on extensive empirical observations, conducted in representative locations that are characteristic for the major physiographic units in Alaska.

The numerical solution of heat transfer is implemented in the extended program module, which can be called from the GIS environment. GIS allows visualization of input and output parameters and their representation in the form of digital maps. The new version of GIPL 2.0 simulates soil temperature and liquid water content fields for the entire spatial domain with daily, monthly and yearly resolution. The merge of the new GIPL and the GIS technique provides a unique opportunity to analyze spatial features of permafrost dynamics with high temporal resolution.

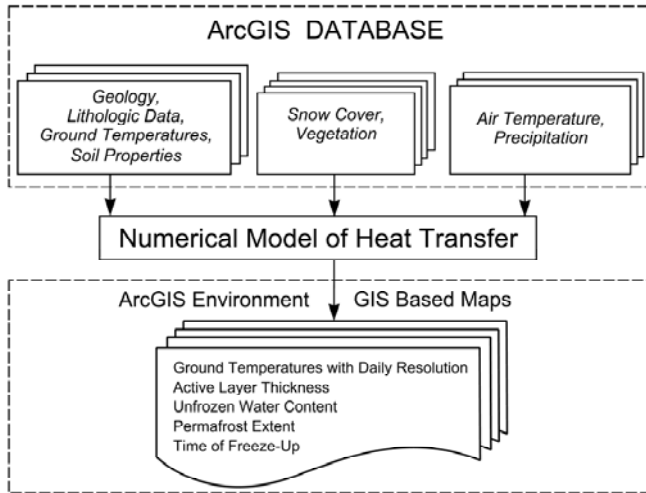


Figure 1. The GIPL-2.0 model schematic diagram.

Mathematical model

The basic mathematical model in our approach is the Enthalpy formulation of the one-dimensional Stefan problem (Alexiades & Solomon 1993, Verdi 1994). We used the quasi-linear heat conduction equation, which expresses the energy conservation law:

$$\frac{\partial H(y,t)}{\partial \tau} = \text{div}(\lambda(y,t)\nabla t(y,\tau)), \quad y \in \Omega, \tau \in \Psi \quad (1)$$

where $H(y, t)$ is the enthalpy

$$H(y,t) = \int_0^t C(y,s)ds + L\Theta(y,t) \quad (2)$$

$C(y, t)$ is the heat capacity, L is the latent heat, $\lambda(y, \tau)$ is thermal conductivity and $\Theta(y, t)$ is the volumetric unfrozen water content. The Equation (1) is complemented with boundary and initial conditions. The computational domain $0 \leq \Omega \leq 1000$ extended to 1000 m in depth, and time interval Ψ is 200 years with initial temporal step of 24 hours.

Dirichlet's conditions $t(\tau)$ were set at the upper boundary. An empirical method of geothermal heat flux estimating (Pollack et al. 1993) in each grid point was applied for the lower boundary conditions.

$$\left. \frac{\partial t}{\partial \tau} \right|_{y=0} = t(\tau), \quad \left. \frac{\partial t(\tau)}{\partial y} \right|_{y=1000} = g \quad (3)$$

where g is a geothermal gradient at the lower boundary.

A fractional step approach (Godunov splitting) was used to obtain a finite difference scheme (Marchuk 1975). The idea is to divide each time step into two steps. At each step along the spatial dimension (in the depth) is treated implicitly:

$$\frac{H(t_i^{n+1}) - H(t_i^{n+1/2})}{\Delta \tau_n} = \frac{2}{(\Delta h_{i+1} + \Delta h_i)} \times \left(\lambda_{i+1/2}^{n+1} \frac{(t_{i+1}^{n+1} - t_i^{n+1})}{\Delta h_{i+1,y}} - \lambda_{i-1/2}^{n+1} \frac{(t_i^{n+1} - t_{i-1}^{n+1})}{\Delta h_{i,y}} \right) \quad (4)$$

where $\Delta h_{i,y}$ is the spatial steps on the non-uniform grid.

The resulting system of finite difference equations is non-linear, and to solve it, the Newton's method was employed at each time step. On the first half step (4) in case when a non-zero gradient of temperature exist, we use the difference derivative of enthalpy:

$$\frac{\partial H(t_i)}{\partial t} = 0.5 \left[\frac{H(t_i) - H(t_{i-1})}{(t_i - t_{i-1})} + \frac{H(t_{i+1}) - H(t_i)}{(t_{i+1} - t_i)} \right] \quad (5)$$

The analytical derivative of representation (2) has to be used in case of zero-gradient temperature fields. Second half step (4) is treated similarly. Thereby, we can employ any size spatial steps without any risk to lose any latent heat effects within the phase transition zone for the fast temporally and spatially varying temperature fields.

Model validation and calibration

Ground temperature measurements of a very high quality (precision generally at 0.01°C) in shallow boreholes were

used for initial model validation. More than 15 shallow boreholes (1-1.2 m in depth) across Alaska from north to south were available for validation (Romanovsky & Osterkamp 1997). The temperature measurements in the shallow holes performed with vertical spacing of 0.08-0.15 m. At most of these sites, soil water content and snow depth also were recorded. In addition, more than 25 relatively deep boreholes from 29 m to 89 m in depth (Osterkamp & Romanovsky 1999, Osterkamp 2003) along the same transect were available for the model validation in terms of permafrost temperature profiles and permafrost thickness.

Different earth's materials have varying thermal properties. The soil thermal conductivity and heat capacity vary within the different soil layers as well as during the thawing/freezing cycles and depend on the unfrozen water content that is a certain function of temperature. The method of obtaining these properties is based on numerical solution for a coefficient inverse problem and on minimization locally the misfit between measured and modeled temperatures by changing thermal properties along the direction of the steepest descent. The method used and its limitations are described in more detail elsewhere (Nicolosky et al., in review).

There are two basic approaches to the calibration of modeled permafrost temperatures against the observed data, which can be distinguished by their use of temporal or spatial relationships. With the temporal approach, the quality of the modeling series is assessed by time series regression against measured data. The quantitative relationship between simulated and measured data is then determined for a "calibration" period with some instrumental data withheld to assess the veracity of the relationship with independent data. Figure 2 illustrates the results of the model calibration for the specific site West Dock (70° 22' 28.08" N, 148° 33' 7.8" W).

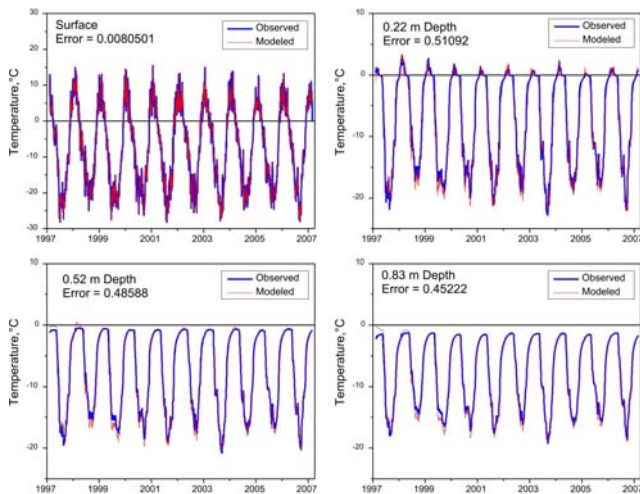


Figure 2. Example of the temporal model calibration for specific site.

In the spatial approach, assemblages of the observed data from a number of different geographic locations with different landscape settings determine the quality of the

modeling results. To achieve geographic correspondence between the scale of observation and modeling we utilized a regional-scale permafrost characterization based on observations obtained from representative locations. Additional comparison of model-produced ground temperatures, active layer thickness and spatial permafrost distribution with measured ground temperatures at the Alaskan sites shows a good agreement.

Input data set

In order to assess possible changes in the permafrost thermal state and the active layer depth, the GIPL-2.0 model was implemented for the entire Alaskan permafrost domain for the 1900-2100 time interval. For this study we used an input data set with grid boxes size $0.5^\circ \times 0.5^\circ$. Input parameters to the model are spatial datasets of mean monthly air temperature and snow water equivalent (SWE), prescribed soil thermal properties and water content, which are specific for each soil layer and for each geographical location. Initial distribution of temperature with depth was derived from the borehole temperature measurements obtained in Alaska by different researchers during the last several decades (Brewer 1958, Lachenbruch & Marshall 1986, Osterkamp & Romanovsky 1999, Clow & Urban 2002, Osterkamp 2003, Osterkamp 2005). As a climate forcing we used two data sets. For the period of 1900-2000 climatic conditions, the CRU2 data set with $0.5^\circ \times 0.5^\circ$ latitude/longitude resolution (Mitchell and Jones 2005) was used. The future climate scenario was derived from the MIT-2D integrated global system model (IGSM) developed at the Massachusetts Institute of Technology (MIT), which is a two dimensional (zonally averaged) atmospheric model coupled with a diffusive ocean model that simulates the surface climate over the land and ocean for 23 latitudinal bands globally (Sokolov & Stone, 1998). Snow data for the entire simulated period 1900-2100 were derived from the terrestrial ecosystem model (TEM) (Euskirchen et al 2006). We used the MIT-2D output for the 21st century with a doubling gradual increase of atmospheric CO₂ concentration by the end of current century that corresponds to the IPCC SRES emission scenario A1B.

Result and discussion

We compared ground temperatures at the depths of 2 m, 5 m, and 20 m for three snapshots of 2000, 2050 and 2100 (Figure 3). If compared with present-day conditions, the greatest changes in temperatures for the 2050 and 2100 will occur at 2 m depth (Figure 3 A, B, C). Results of calculation show that by the end of the current century, the mean annual ground temperatures (MAGT) at 2 m depth could be above 0°C everywhere southward of sixty-sixth latitude except for the small patches at the high altitudes of the Alaska Range and Wrangell Mountains (Figure 3C). The area of about 850,000 km² (about of 57% of total area of Alaska) will be involved in the widespread permafrost degradation and could contain both areas with completely disappeared permafrost and the areas where thawing of permafrost is still ongoing. It should be noted that by the term of 'thawing

permafrost' we understand a situation when the permafrost table is lowered down and a residual thawed layer ('talik') between the seasonally frozen layer and permafrost table continuously exists throughout the year.

According to calculations, the modern extent of the area with MAGT at 5 m depth above 0°C is about 125,000 km². The model-produced ground temperatures with positive MAGT at 5 m depth could occupy approximately 659,000 km² (about of 45% of total area of Alaska) by the end of the current century and could extend into the Interior of Alaska (Figure 3F).

While the permafrost temperatures at 20 m depth could change significantly within a range of negative

temperatures, the area with MAGT above 0°C at 20 m depth will not expand too much even by 2100 (Figure 3 G, H, I). The difference between these areas in 2000 and in 2100 does not exceed 100,000 km² (Figure 3 G, I). Changes in permafrost temperatures will be much more pronounced within the areas with colder permafrost in comparison with areas where the permafrost temperature is presently close to 0°C. Also, it will not increase significantly in the areas of peat lands with a sufficiently deep organic layer. Projected changes in area of MAGT above 0°C at the different depths and for the different time accordingly MIT-2D climate change scenario presented in Table 1.

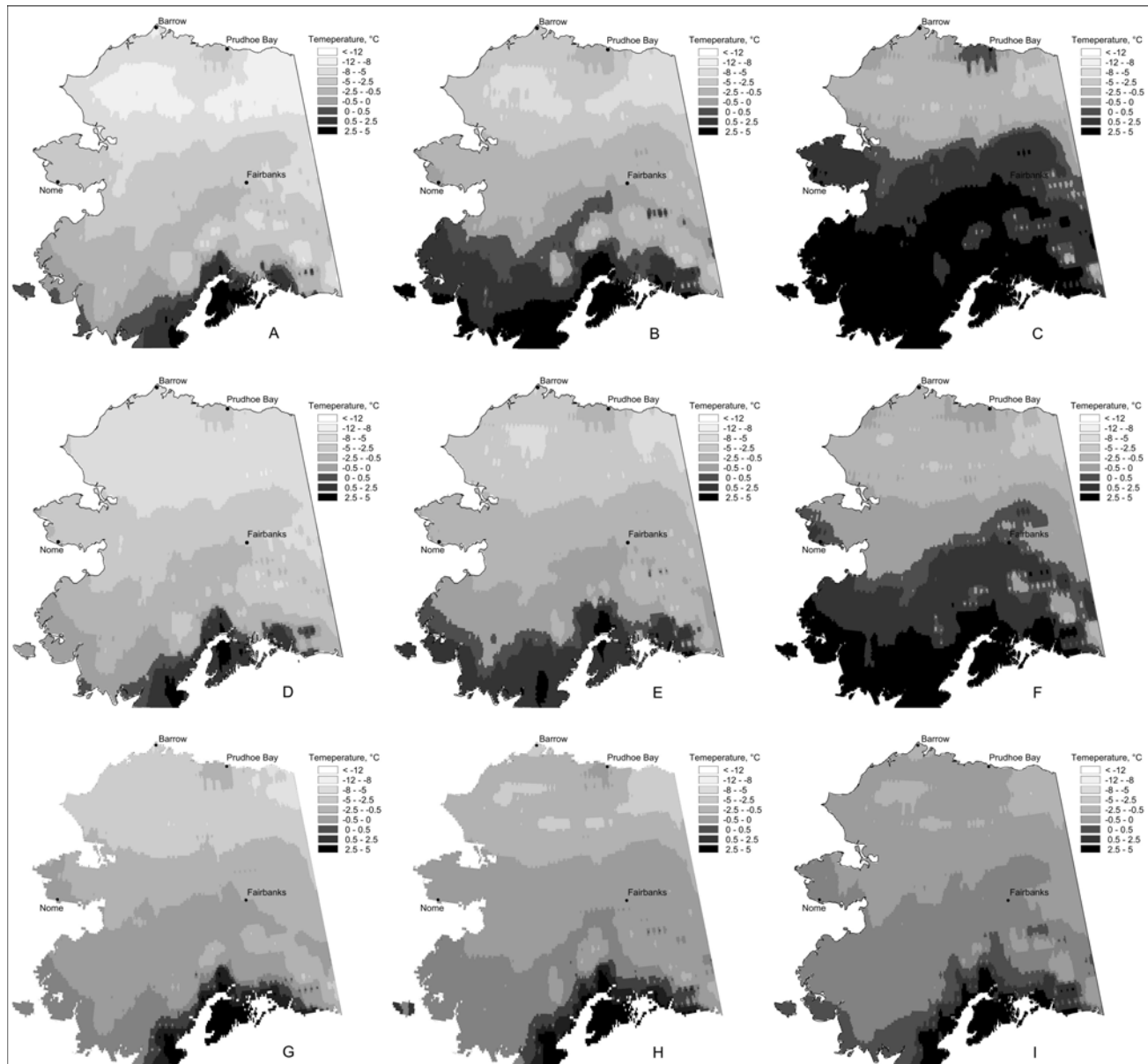


Figure 3. Projected mean annual ground temperatures at 2 m (A, B, C), 5 m (D, E, F), and 20 m (G, H, I) depths on 2000 (A, D, G), 2050 (B, E, H), and 2100 (C, F, I) using climate forcing from MIT-2D output for the 21st century.

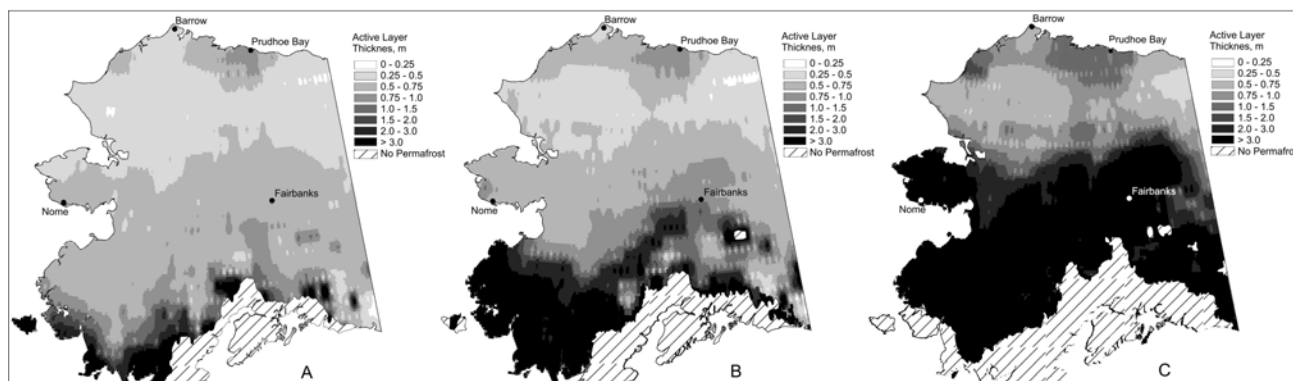


Figure 4. Projected active layer thickness and extent of thawing permafrost area in 2000 (A), 2050 (B), and 2100 (C) using climate forcing from MIT-2D output for the 21st century.

Table 2 presents the statistics of modeled MAGT variables for the three snapshots obtained from 34,434 grid cells within the entire Alaskan domain. While the mean value and sums of MAGT at the depths of 2 m and 5 m turned to above 0°C by the end of current century, the same characteristics for 20 m depth remain below 0°C (Table 2).

Table 1. Areas of simulated MAGT above 0°C at the different depths and for the different time (thousands km²/percent of total area of Alaska).

Depth	2000	2050	2100
2 m	138.8/9.4	410.3/27.8	850.5/57.6
5 m	126.7/8.6	280.2/18.9	658.9/44.6
20 m	103.2/6.7	133.5/9.03	196.4/13.3

Table 2. Statistics of modeled MAGT variables within the entire calculated Alaskan spatial domain (34,434 grid cells).

Statistics	2000	2050	2100
2 m Depth			
Min	-12.52	-8.74	-5.44
Max	4.72	7.30	11.62
Mean	-4.32	-1.47	1.58
5 m Depth			
Min	-8.45	-6.62	-5.43
Max	3.71	5.00	10.46
Mean	-3.69	-1.68	0.54
20 m Depth			
Min	-9.86	-7.74	-5.38
Max	4.85	6.46	8.53
Mean	-3.32	-1.86	-0.62

Statistics on active layer thickness (ALT) also has shown significant response to scenario of climate change. The simulated mean values of ALT for the whole Alaskan permafrost domain are 0.78 m, 1.33 m and 2.4 m for 2000, 2050, and 2100 accordingly.

The area of thawing permafrost (permafrost table located deeper than 3 m) also increased according to our model from 65,000 km² in 2000 to 240,000 km² by 2050 and to 720,000 km² by 2100 (Figure 4).

Conclusions

According to the future climate scenario derived from the MIT-2D climate model and TEM output for the 21st century, a widespread permafrost degradation could be observed everywhere in Alaska southward from the Brooks Range by

the end of the current century. It means that the permafrost table in this region will be lowered down to 3-10 m in depth, and some small and thin patches of permafrost at the southernmost regions of Alaska could disappear completely. Nevertheless, permafrost thicker than 15-20 m in depth could still survive deeper than 10-15 m even in the regions with widespread long-term thawing of permafrost. In the regions with ice-rich permafrost, the thawing processes will extended for a long time, especially in the regions with undisturbed surfaces. Modeling results shows the Alaskan North Slope will be not experiencing a substantial widespread permafrost thawing and degradation during the present century.

Acknowledgments

This research was funded by ARCSS Program and by the Polar Earth Science Program, Office of Polar Programs, National Science Foundation (OPP-0120736, OPP-0352957, OPP-0352958, ARC-0632400, ARC-0520578, ARC-0612533, IARC-NSF CA: Project 3.1 Permafrost Research), by NASA Water and Energy Cycle grant, and by the State of Alaska. We would like to thank Dr. N. Shiklomanov from the University of Delaware helpful discussions. We also like to thank two anonymous reviewers for very helpful suggestions that were used to improve the manuscript.

References

Anisimov OA, Nelson FE. 1997. Permafrost zonation and climate change in the northern hemisphere: results from transient general circulation models. *Climatic Change*. 35: 241–258.

Alexiades, V., & Solomon, A. D. 1993. *Mathematical modeling of melting and freezing processes*, Washington, Hemisphere, 325 pp.

Brewer, M.C., 1958. *Some Results of Geothermal Investigations of Permafrost in Northern Alaska*. Transaction, AGU, 39,19-26.

Burn, C.R., Nelson, F.E. 2006. Comment on “A projection of severe near-surface permafrost degradation during the 21st century” by David M. Lawrence and

- Andrew G. Slater. *Geophysical Research Letters* 33, L21503, DOI:10.1029/2006GL027077.
- Clow, G.D. & Urban, F.E., 2002. Largest permafrost warming in northern Alaska during the 1990s determined from GTN-P borehole temperature measurements. *EOS, Transactions of the AGU* 83 (47), F258.
- Delisle, G. 2007. Near-surface permafrost degradation: How severe during the 21st century? *Geophysical Research Letters* 34, L09503, DOI:10.1029/2007GL029323
- Euskirchen, E.S., McGuire, A.D., Kicklighter, D.W., Zhuang, Q., Klein, J.S., Dargaville, R.J., Dye, D.G., Kimball, J.S., McDonald, K.C., Melillo, J.M., Romanovsky, V.E. and Smith, N.V. 2006. Importance of Recent Shifts in Soil Thermal Dynamics on Growing Season Length, Productivity, and Carbon Sequestration in Terrestrial High-Latitude Ecosystems. *Global Change Biology*. 12: 731-750.
- Harris, C. & Haeberli, W. 2003. Warming permafrost in European mountains. *World Meteorol. Org. Bull.*, 52(3), 6 (See also *Global and Planetary Change*, 39: 215–225).
- Jin H., Li S., Cheng G., Shaoling W. & Li X., 2000. Permafrost and climatic change in China. *Global and Planetary Change*, 26(4): 387-404.
- Lachenbruch, A.H. & Marshall, B.V. 1986. Changing climate: Geothermal evidence from permafrost in the Alaskan Arctic. *Science*. 234: 689–696.
- Lawrence, D. M., and A. G. Slater. 2005. A projection of severe nearsurface permafrost degradation during the 21st century. *Geophys. Res. Lett.*, 32, L24401, doi:10.1029/2005GL025080.
- Marchenko, S., Gorbunov, A. & Romanovsky, V. 2007. Permafrost Warming in the Tien Shan Mountains, Central Asia. *Global and Planetary Change*, 56: 311-327.
- Marchuk, G.I. 1975. *Methods of Numerical Mathematics (Applications of Mathematics)*. New York, Springer-Verlag, 316 pp.
- Mitchell, T. D. and Jones, P.D. 2005. An improved method of constructing a database of monthly climate observations and associated high-resolution grids. *International Journal of Climatology*. 25(6): 693-712.
- Nicolosky, D.J., Romanovsky, V.E. & Tipenko, G.S. Estimation of thermal properties of saturated soils using in-situ temperature measurements. *The Cryosphere*, 1, 41–58, 2007.
- Nicolosky, D. J., V. E. Romanovsky, V. A. Alexeev, and D. M. Lawrence. 2007. Improved modeling of permafrost dynamics in a GCM land-surface scheme. *Geophys. Res. Lett.*, 34, L08501, doi:10.1029/2007GL029525.
- Oberman, N.G. & Mazhitova, G.G., 2001. Permafrost dynamics in the northeast of European Russia at the end of the 20th century. *Norwegian Journal of Geography*, 55: 241-244.
- Oelke, C., and T. Zhang. 2004. A model study of circum-Arctic soil temperatures, *Permafrost Periglacial Processes*, 15, 103–121.
- Osterkamp, T.E. & Romanovsky, V.E. 1999. Evidence for Warming and Thawing of Discontinuous Permafrost in Alaska. *Permafrost and Periglacial Processes*, 10: 17-37.
- Osterkamp, T.E. 2003. Establishing Long-term Permafrost Observatories for Active-layer and Permafrost Investigations in Alaska: 1977–2002. *Permafrost and Periglacial Processes*. 14: 331–342.
- Osterkamp, T.E. 2005. The recent warming of permafrost in Alaska, *Global and Planetary Change*. 49: 187–202.
- Pollack, H.N., Hurter, S.J., & Johnson, J.R., 1993. Heat flow from the earth's interior: analysis of the global data set, *Reviews of Geophysics* 31(3), 267-280.
- Romanovsky, V.E. and Osterkamp, T.E. 1997. Thawing of the active layer on the coastal plain of the Alaskan Arctic, *Permafrost and Periglacial Processes*, 8(1): 1-22.
- Romanovsky, V., Burgess, M., Smith, S., Yoshikawa, K. & Brown, J., 2002. Permafrost Temperature Records: Indicators of Climate Change, *EOS, AGU Trans.*, 83(50): 589-594.
- Romanovsky, V.E., Sazonova, T.S., Balobaev, V.T., Shender, N.I., and D.O. Sergueev, 2007. Past and recent changes in permafrost and air temperatures in Eastern Siberia, *Global and Planetary Change*, 56: 399-413.
- Saito, K., Kimoto, M., Zhang, T., Takata, K., and Emori, S. 2007. Evaluating a high-resolution climate model: Simulated hydrothermal regimes in frozen ground regions and their change under the global warming scenario. *J. Geophys. Res.*, 112, F02S11.
- Sazonova, T. S. and V. E. Romanovsky, A Model for Regional-Scale Estimation of Temporal and Spatial Variability of the Active Layer Thickness and Mean Annual Ground Temperatures, *Permafrost and Periglacial Processes*, 14(2): 125-139, 2003
- Sharkhuu, N. 2003. Recent Changes in permafrost of Mongolia. *Proceedings of the 8th International Conference on Permafrost, Zurich, Switzerland, July 2: 1029-1034.*
- Sokolov, A.P. and Stone, P.H. 1998. A flexible climate model for use in integrated assessments. *Climate Dynamics*. 14: 291-303.
- Stendel, M. and Christensen, J.H. 2002. Impact of global warming on permafrost conditions in a coupled GCM. *Geophysical Research Letters*, 29(13), 1632, 10.1029/2001GL014345,
- Verdi, C. 1994. Numerical aspects of parabolic free boundary and hysteresis problems. *Lecture Notes in Mathematics*, New York, Springer-Verlag, 213-284.
- Zhang, Y., W. Chen, and Riseborough, D.W. 2006. Temporal and spatial changes of permafrost in Canada since the end of the Little Ice Age, *J. Geophys. Res.*, 111, D22103, doi:10.1029/2006JD007284.